X-Ray Diffraction Studies of Cross-Bridges Weakly Bound to Actin in Relaxed Skinned Fibers of Rabbit Psoas Muscle

S. Xu,* S. Malinchik,* D. Gilroy,* Th. Kraft,* B. Brenner,# and L. C. Yu*
*National Institutes of Health, Bethesda, Maryland 20892 USA, and #Hannover Medical School, Hannover, Germany

ABSTRACT X-ray diffraction patterns were obtained from skinned rabbit psoas muscle under relaxing and rigor conditions over a wide range of ionic strengths (50–170 mM) and temperatures (1°C–30°C). For the first time, an intensification of the first actin-based layer line is observed in the relaxed muscle. The intensification, which increases with decreasing ionic strength at various temperatures, including 30°C, parallels the formation of weakly attached cross-bridges in the relaxed muscle. However, the overall intensities of the actin-based layer lines are low. Furthermore, the level of diffuse scattering, presumably a measure of disorder among the cross-bridges, is little affected by changing ionic strength at a given temperature. The results suggest that the intensification of the first actin layer line is most likely due to the cross-bridges weakly bound to actin, and that the orientations of the weakly attached cross-bridges are hardly distinguishable from the detached cross-bridges. This suggests that the orientations of the weakly attached cross-bridges are not precisely defined with respect to the actin helix, i.e., nonstereospecific. Intensities of the myosin-based layer lines are only marginally affected by changing ionic strength, but markedly by temperature. The results could be explained if in a relaxed muscle the cross-bridges are distributed between a helically ordered and a disordered population with respect to myosin filament structure. Within the disordered population, some are weakly attached to actin and others are detached. The fraction of cross-bridges in the helically ordered assembly is primarily a function of temperature, while the distribution between the weakly attached and the detached within the disordered population is mainly affected by ionic strength. Some other notable features in the diffraction patterns include a ≈1% decrease in the pitch of the myosin helix as the temperature is raised from 4°C to 20°C.

INTRODUCTION

It is generally accepted that force is generated by the cyclic interactions between myosin and actin during the hydrolysis of ATP. The actomyosin interaction alternates between two groups of states, known as "weak-binding" and "strong-binding" states (Eisenberg and Hill, 1985). Cross-bridges in the weak-binding states are characterized by their low affinity to actin and their inability to activate the thin filaments; those in strong-binding states are characterized by their higher actin affinity and their ability to activate the thin filaments.

The existence of the weakly bound cross-bridges has been experimentally confirmed in skinned, relaxed rabbit psoas muscle fibers (Brenner et al., 1982, 1984, 1991; Kraft et al., 1995), frog muscles (Xu et al., 1987; Schoenberg, 1988), and insect flight muscle (Granzier and Wang, 1993). More significantly, it was demonstrated that force production can only occur after the cross-bridges have first attached to actin in a weakly bound configuration (Brenner et al., 1991; Kraft et al., 1995). It was proposed that a major element in force generation is a structural change in the orientation/attitude of the attached cross-bridges in transition from the weakly bound configuration to the force-generating configuration. As a first step in understanding the structural basis of contraction, studies of the weakly bound cross-bridges in relaxed muscle fibers are therefore essential.

The structure of weakly bound cross-bridges in relaxed muscle has been studied previously (Matsuda and Podolsky, 1984; Xu et al., 1987). It was shown by Matsuda and Podolsky that in the two-dimensional x-ray diffraction patterns, the formation of the weakly attached cross-bridges in the relaxed muscle fibers had little effect on the myosin-based layer lines, whereas in rigor fibers with the cross-bridges strongly bound, these layer lines were greatly weakened and the actin-based layer lines were greatly enhanced. These results and those obtained by equatorial x-ray diffraction (Brenner et al., 1984; Yu and Brenner, 1989) suggested that the structure of the weak attachment differed significantly from the strong attachment. However, the diffraction patterns recorded by Matsuda and Podolsky showed some features that are associated with rigor conditions. It is not clear whether such features reflect the structures of the weakly bound cross-bridges or are due to a mixed population of weakly bound and rigor cross-bridges present in the muscle during experiments. In addition, due to technical limitations, detailed analysis of the diffraction patterns was not possible.

We have recorded two-dimensional diffraction patterns of bundles of chemically skinned rabbit psoas muscle fibers at various ionic strengths and at different temperatures,

Received for publication 10 February 1997 and in final form 4 August 1997.

Address reprint requests to Dr. L. C. Yu, NIAMS, the National Institutes of Health, Bldg. 6, Room 114, Bethesda, MD 20892-2775. Tel.: 301-496-5415; Fax: 301-402-0009; E-mail: lcyu@helix.nih.gov.

Dr. Malinchik's present address is Boston College, Chestnut Hill, MA 02167.

Dr. Gilroy's present address is University of North Carolina Hospitals, Chapel Hill, NC 27834.

Dr. Kraft's present address is Hannover Medical School, Hannover, Germany.

0006-3495/97/11/2292/12 $2.00

using synchrotron x-ray radiation and imaging plate detector systems. Careful control of muscle conditions, short exposure time, and digital recording instrumentation made it possible to analyze the structure of the weakly bound state of cross-bridges with improved resolution. The present results show that diffraction patterns from relaxed muscle fibers with various fractions of cross-bridges weakly attached are devoid of features associated with rigor conditions. The attachment orientations are most likely nonstereospecific. In an accompanying paper (Malinchik et al., 1997), the structure of the myosin filament helix as a function of temperature is analyzed quantitatively by modeling.

Preliminary results have been presented earlier (Xu et al., 1996; Malinchik et al., 1996).

METHODS

Muscle preparation and solutions

All experiments were performed on chemically skinned bundles of the rabbit M psoas major. Bundles of 1 mm × 2 mm in cross-section were first chemically skinned according to Kraft et al. (1995). Each large bundle consisted of many small single bundles ~0.3 mm × 0.6 mm in size that are naturally separated from one another by connective tissue. The small bundles, ~30 mm in length, were dissected out singly, such that each bundle was not stretched more than 20% of the rest length during dissection procedures. The skinning solution was renewed every 24 h. No bundles older than 3 days were used.

The following solutions were used for the experiments: 1) Relaxing solution contained (mM): 2 MgATP, 2 $MgCl_2$, 2 EGTA, 2 DTT, 10 imidazole, pH 7.0, μ = 27 mM. In the experiments using synchrotron radiation the solution with an extra 3 mM DTT and 1200 units/ml catalase was used for better protection from radiation damages. Ionic strength ranged between 50 and 170 mM, which was adjusted by adding various amounts of creatinephosphate (CrP). To complete the ATP-backup system, 440 units/ml of CPK was added just before the x-ray experiments. 2) Rigor solution contained (mM): 2.5 EGTA, 2.5 EDTA, 10 imidazole, pH 7.0. Ionic strength for the rigor solution was adjusted by adding various amounts of potassium propionate and ranged between 50 mM and 170 mM. Before applying the rigor solution, the bundles were always rinsed several times by a "quick rinse" solution containing (mM): 5 EGTA, 15 EDTA, 20 imidazole, pH = 7.0, μ = 70 mM (Brenner et al., 1986; Brenner and Yu, 1991).

Sarcomere length was adjusted to 2.5 μm at the dissecting table by light diffraction. During the entire course of the experiments, the solution in the chamber was continuously stirred by a syringe pump at the rate of ~1 ml/s to minimize any gradient (e.g., temperature gradient) along the length of the bundles. To reduce radiation damage, the specimen chamber was moved up and down continuously for a range of 6 mm at a constant rate of 4 mm/s by a stepping motor (Aerotech, Pittsburgh, PA).

Tension was monitored by means of a displacement transducer (Yu et al., 1979). The tension level of each bundle in the skinning solution (μ = 180 mM) at 4°C was defined as zero. Only the data from bundles with measurable tension of <2% (<40 mg for a 0.3 mm × 0.6 mm bundle) of the estimated maximal active force were included in the final analysis.

X-ray camera and imaging plate detector system

Initially the experiments were performed in the laboratory at the National Institutes of Health using a rotating anode x-ray generator (Elliott GX-6). The x-ray beam was focused by a double-mirror Franks camera. Sample-to-detector distance was 89 cm. Approximately 85% of the x-ray path was filled with helium. The two-dimensional x-ray patterns were recorded on a MAR Research imaging plate detector system (X-ray Research GmbH, Hamburg, Germany). Pixel size was specially modified to 50 μm × 50 μm. The scanning area was 10 cm in diameter.

The layer line intensities of the relaxed fibers are very weak, particularly at low temperatures. To obtain sufficient counting statistics while maintaining the viability of the muscle preparation, at the final stage of this series of experiments we used the synchrotron radiation at Deutches Electronen Synchrotron (DESY), Hamburg, Germany as the x-ray source. Beamline X13 of European Molecular Biology Laboratory (EMBL) was specially designed for small specimens. The size of the x-ray beam at the specimen was adjusted to be ~1 mm × 1.7 mm and the focal spot was 0.5 mm × 1.5 mm. The camera length was 284 cm. Fuji imaging plates (Fuji, Japan) were used to record the diffraction patterns and a BAS2000 scanner was used to scan the imaging plates at 100 × 100 μm pixel size. Exposure time for each pattern was 4 min or less. The maximum accumulated exposure time on each bundle was <20 min. Most of the diffraction patterns shown in this paper were obtained by using the synchrotron radiation source at DESY.

Experimental protocol

To compare directly the intensities obtained under several different conditions with minimal error, diffraction patterns were always recorded from the same bundles for all the conditions of interest. For better data statistics, entire sets of exposures were performed on different bundles with various permutations of the conditions. The patterns recorded under each condition were subsequently added together to raise the signal-to-noise ratio (see Data Analysis below).

Data reduction and analysis

The data were displayed and analyzed on Silicon Graphics Indigo workstations (Mountain View, CA) using a software program, Profida, originally written by M. Lorenz of Max Plank Institut of Heidelberg, Germany. The program was modified to suit the size of the current data (up to 2000 × 2000 pixels) and wider dynamic range. In addition, the current program uses a different approach for rotating and translating the x-ray patterns to ensure that the meridian is vertical and the center of the diagram is on the origin of the Cartesian coordinates. The algorithm for rotation and translation is based on properly orientating and locating the reflection peaks on the equator (e.g., [1, 0]) and on the meridian (e.g., $1/143$ Å^{-1}). Data analysis includes the following procedures. The patterns of the original data were first rotated and translated. The data in the four quadrants were added (folded) and averaged. For the patterns obtained in Hamburg, there was a beam stop present in one of the quadrants. Only the remaining three quadrants were averaged. After averaging, integrated intensity profiles were taken. The width of the slices were chosen to include the whole reflection areas.

For analysis of radial distributions of intensities and spacings of weak layer lines, a set of contiguous axial slices was defined perpendicular to the layer lines. [Throughout this paper, "axial" direction is defined to be parallel to the meridian; "radial" direction, parallel to the equator.] Within each slice (generally 0.001 Å^{-1} in width), the background was subtracted using the PCA program (Nucleus, Oak Ridge, TN) by interpolating linearly in the region of maxima. Intensities above the background were then integrated. These slices cover a region in the radial direction approximately from center to $1/100$ Å^{-1}. The integrated intensities of the layer line segments and their axial centroid positions were used to reconstruct the intensity profiles of the individual layer lines along the radial direction.

Calibration of spacings

The spacings of all reflections are calibrated by the reflection at [1/144.3] Å^{-1} on the meridian from the skinned rabbit psoas muscle in rigor at μ = 170 mM and T = 20°C. The reflection at 151 Å was not included in the measurement. This value of 144.3 Å was first reported by Huxley and Brown (1967), and was confirmed in our experiments by comparing the

spacings of that reflection from the skinned rabbit muscle in rigor and from the resting frog sartorius muscle at [1/143.4] $Å^{-1}$.

RESULTS

Two-dimensional x-ray diffraction patterns from bundles of rabbit muscle fibers in relaxed or rigor conditions at several ionic strengths (from 50 mM to 170 mM) and at several temperatures (from 1°C to 30°C) were systematically obtained. The typical patterns are shown in Fig. 1. In general, the skinned fiber bundles yielded 2D diffraction patterns with well defined myosin-based layer lines under relaxing conditions, and well defined actin-based layer lines under rigor conditions. The patterns under relaxing conditions exhibit strong temperature dependence, as previously reported by Wray (1987), Wakabayashi et al. (1988), and Lowy et al. (1991).

Equatorial intensities and lattice spacings

Comparison between single fibers and single bundles under the same conditions

One of the concerns of the multi-fiber preparations is that there might be ATP depletion at the core region of the bundle due to limited diffusion. To ensure that the bundle was fully relaxed under conditions of interest, we compared the equatorial diffraction patterns from the bundles and the single fibers by obtaining diffraction patterns under the same conditions (i.e., the same solution, temperature, and sarcomere length) for both preparations.

Profiles along the equator of the two-dimensional patterns were made with an axial width of 0.00303 $Å^{-1}$ that covered the height of the [1, 1] reflection peak area. The equatorial profiles for the two preparations were found to be

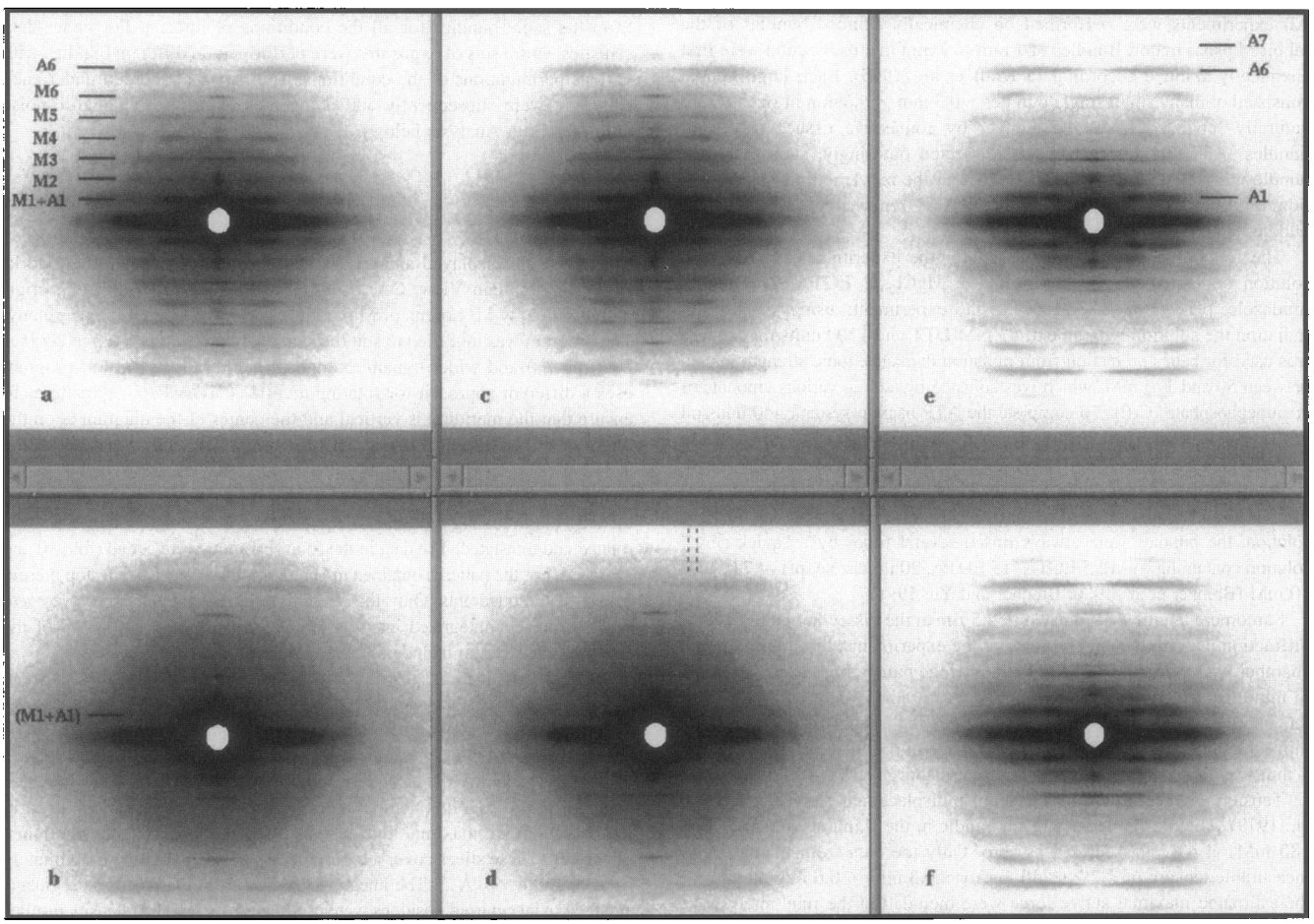

FIGURE 1 X-ray diffraction patterns from single bundles of skinned rabbit psoas muscle fibers. (*a*) In relaxing solution with ionic strength μ = 150 mM at T = 20°C. (*b*) In relaxing solution, μ = 150 mM, T = 4°C. (*c*) In relaxing solution, μ = 50 mM, T = 20°C. (*d*) In relaxing solution, μ = 50 mM, T = 4°C. (*e*) In rigor solution, μ = 170 mM, T = 20°C. (*f*) In rigor solution, μ = 170 mM, T = 4°C. Original patterns were obtained by using synchrotron radiation on beamline X13 of EMBL at DESY, Hamburg, Germany. The images were recorded on Fuji imaging plates with 100 μm × 100 μm pixel size. The camera length was 284 cm and exposure time for each pattern was 4 min. The patterns were rotated and then averaged with three quadrants. All patterns shown here were normalized by the integrated intensities of the equatorial [10] reflection of the bundles in the relaxing solution 50 mM and at 4°C. The patterns are displayed in logarithmic scale. (*a*) and (*c*) were averaged patterns from 3 sets of experiments with random sequence of conditions. (*b*) and (*d*) were averaged patterns from two sets of experiments. (*e*) and (*f*) from the same single bundle. The *dotted lines* in (*d*) show a typical width of axial slices used for analysis.

closely comparable at both low (50 mM) and high (170 mM) ionic strengths, as shown in Fig. 2.

The equatorial intensities at 4°C generally agree with our earlier results, i.e., the magnitude of decrease in I_{10} is proportionately less than the increase in I_{11} as the ionic strength is reduced. The present data further showed that at high temperature (20°C), I_{10} is even less sensitive to changes in ionic strength, whereas I_{11} increases considerably with lowering of ionic strength (Table 1).

The lattice spacing d_{10} increases with ionic strength as reported earlier (Brenner et al., 1984; Yu and Brenner, 1989). When the temperature is raised from 4°C to 20°C, however, the d_{10} *decreases* by ~20 Å at the same ionic strengths.

Although muscle bundles are highly susceptible to ATP depletion under low ionic strength conditions, these parallel experiments, together with the continuous monitor of tension, led us to conclude that the bundles were fully relaxed under all the relaxing conditions used in this study.

Layer lines

High-resolution 2D patterns were obtained by using the EMBL synchrotron radiation source at DESY (Fig. 1). The patterns from relaxed muscles at 20°C and 30°C, regardless of ionic strength, show strong myosin-based layer lines, indicating well-ordered thick filament helical structures (Fig. 1 , *a* and *c*). The patterns from relaxed muscle at 4°C were significantly weaker, but at least five myosin-based layer lines were clearly visible (Fig. 1 , *b* and *d*). As an example, the integrated intensities within an axial slice (0.001 $Å^{-1}$ in width) centered at the peak of the 5th myosin-based layer line is shown in Fig. 3. In general, at 4°C the intensities of myosin-based layer lines decrease somewhat (between 10% and 20%) with increasing ionic strength. The change is hardly detectable at 20°C.

Detailed analysis of the changes of myosin-based layer lines as a function of temperature and modeling of the structures will be found in the accompanying paper (Malinchik et al., 1997).

The profile of the sixth actin layer line (59 Å) is shown in Fig. 4. As it was reported previously by Matsuda and Podolsky (1984), the intensity distribution of this layer line under relaxing condition is not affected by ionic strength, whereas in rigor, it is greatly enhanced and the peak position is shifted toward the center.

Centroid position of the first layer line in the axial direction

The first layer line ("M + A" in Fig. 1) in the diffraction patterns from the relaxed muscle is the strongest among all layer lines. Upon close examination, it is revealed that along "M + A", the axial centroid gradually changes with distances

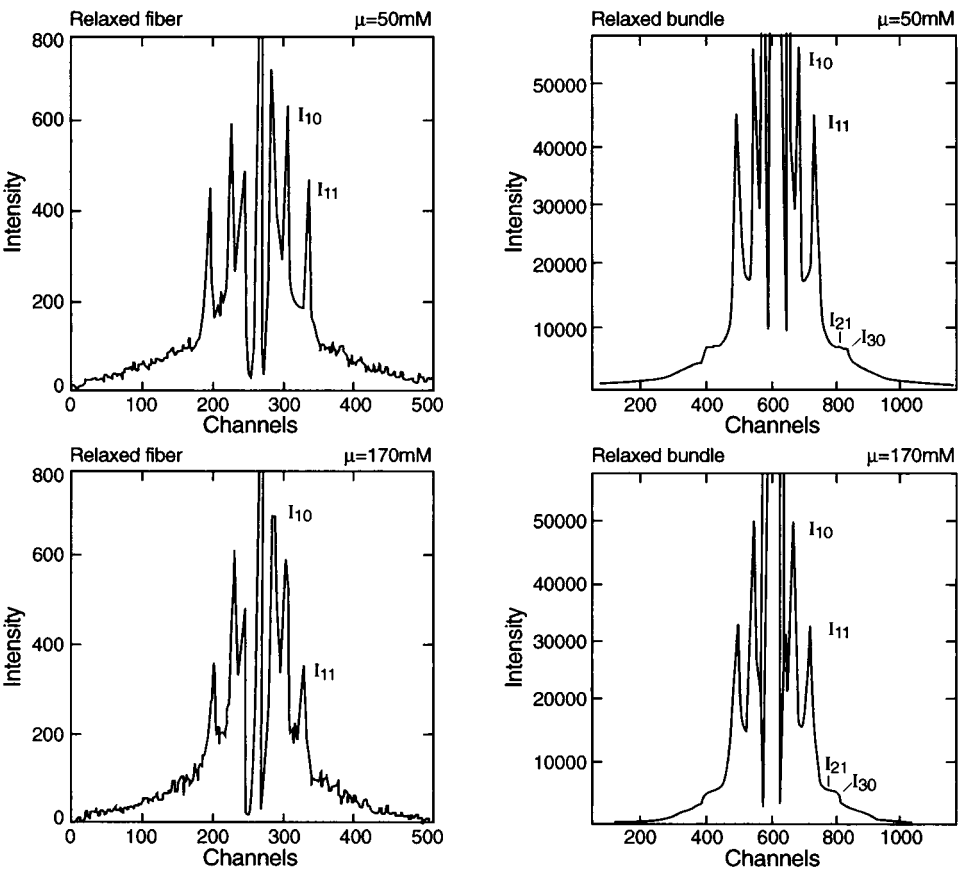

FIGURE 2 Equatorial intensities from a single fiber compared with those from a single bundle of fibers at ionic strengths of 50 mM and 170 mM. The patterns (*left*) of a single fiber (~80 μm in diameter) were obtained using a wire position-sensitive detector in the laboratory (Ordela, Oak Ridge, TN). Exposure time was 500 s. Diffraction patterns (*right*) from the bundles were also obtained in the laboratory using an MAR Research imaging plate system. Exposure time was 1 h.

TABLE 1 Intensities and spacings of equatorial reflections from skinned fiber bundles

Conditions	T (°C)	μ (mM)	I_{11}/I_{10}	I_{11}	I_{10}	d_{10} (Å)	d_{11} (Å)
Relaxed*	4	50	1.53	153	100	400	229
Relaxed#	4	150	0.98	116	118	418	240
Relaxed§	20	50	0.55	82	148	380	218
Relaxed¶	20	150	0.29	43	147	396	227
Rigor	20	170	2.11	149	71	386	223
Rigor	4	170	2.12	172	81	388	223

*Average of two bundles.
#Average of the same bundles as in (*).
§Average of three bundles.
¶Average of the same three bundles as in (§).

from the meridian. The changes determined at different ionic strengths at 4°C and 20°C are shown in Fig. 5, *A* and *B*. The temperature effects at μ = 50 mM are shown in Fig. 5 *C*.

For the relaxed muscle at 4°C, the axial centroid is at 1/428 Å^{-1} in the radial region from 1/500 to 1/250 Å^{-1}. After 1/250 Å^{-1}, it shifts toward a spacing approaching 365 Å. At 20°C, the axial centroid of the first layer line remains at ~1/422 Å^{-1} in the radial region from 1/500 to 1/140 Å^{-1}, and starts to shift toward 1/365 Å^{-1} after the radial distance is >1/140 Å^{-1}. It is clear from Fig. 5 that under all relaxing conditions studied, the axial centroid of the first layer line shifts from a myosin filament-based spacing toward an actin filament-based spacing at larger distances from the meridian. Second, the lower the ionic strength of the relaxing solution, the greater the shift toward the actin-based spacing.

In contrast, for the rigor muscle at 4°C, 20°C, and 30°C, the centroid of the first layer line remains at 1/366 Å^{-1} within the radial distances ranging from 1/240 to 1/110 Å^{-1}.

Diffuse scattering from the muscle fibers

The extent of diffuse scattering observed in the present study displays a pattern similar to those reported by Lowy et al. (1991), i.e., it is approximately in a diamond shape. The extent in the equatorial direction is greater than that in the meridional direction. The level of the diffuse scattering varies greatly with experimental conditions (Fig. 1). Fig. 6 shows the profiles of the intensities along the meridian of the diffraction patterns from the same bundles of fibers under various conditions. The patterns were recorded within a short period of time where the camera conditions remained constant. Thus, it is reasonable to assume that the change in the background of the profiles under the relaxing conditions is a measure of changes in the diffuse scattering from the muscle fibers alone, since the solution remained the same. At a given temperature, the background level is little affected by ionic strength, although it is somewhat lower as ionic strength is changed from 150 mM to 50 mM at 4°C (Fig. 6 *A*). Similar differences in the background level are observed in the off-meridional regions between R = 0.0023 Å^{-1} and 0.014 Å^{-1} (profiles not shown).

Control experiments indicated that approximately one-half of the difference in the background in the region of the "143 Å" (M3) reflections under the relaxing condition at

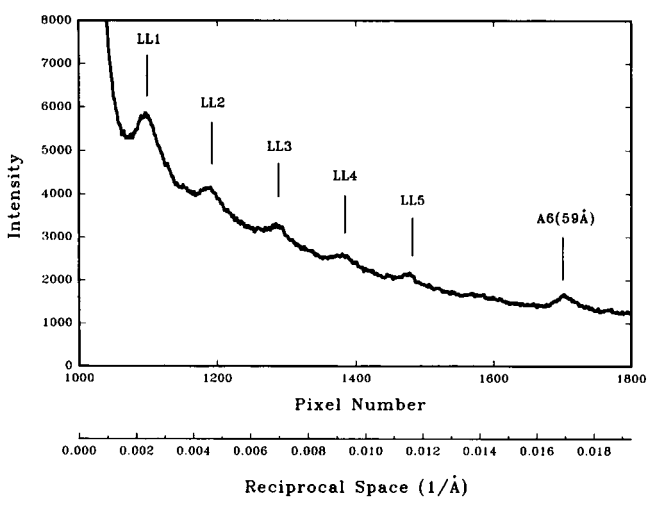

FIGURE 3 Profile from an axial slice centered at the reflection peak of the 5th myosin layer line from a relaxed bundle at μ = 50 mM, T = 4°C (see the dotted lines in Fig. 1 *d*). Reflections from myosin-based layer lines one through five and actin-based 59 Å layer line (A6) can be seen clearly.

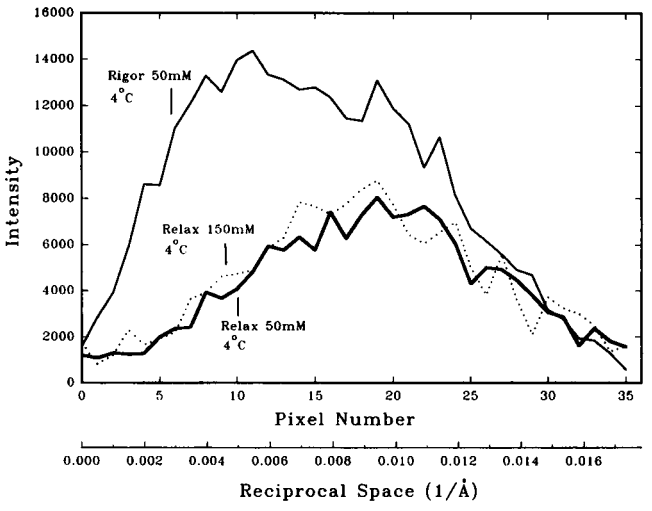

FIGURE 4 Intensity distribution along the sixth actin-based layer line (59 Å). *Thin solid line*, under rigor at μ = 50 mM; *dotted line*, relaxed at μ = 150 mM; *thick solid line*, relaxed at μ = 50 mM. T = 4°C. Profiles were reconstructed from integrated intensities in 35 contiguous axial slices 0.0005 Å^{-1} in width. The data were obtained from the same bundle.

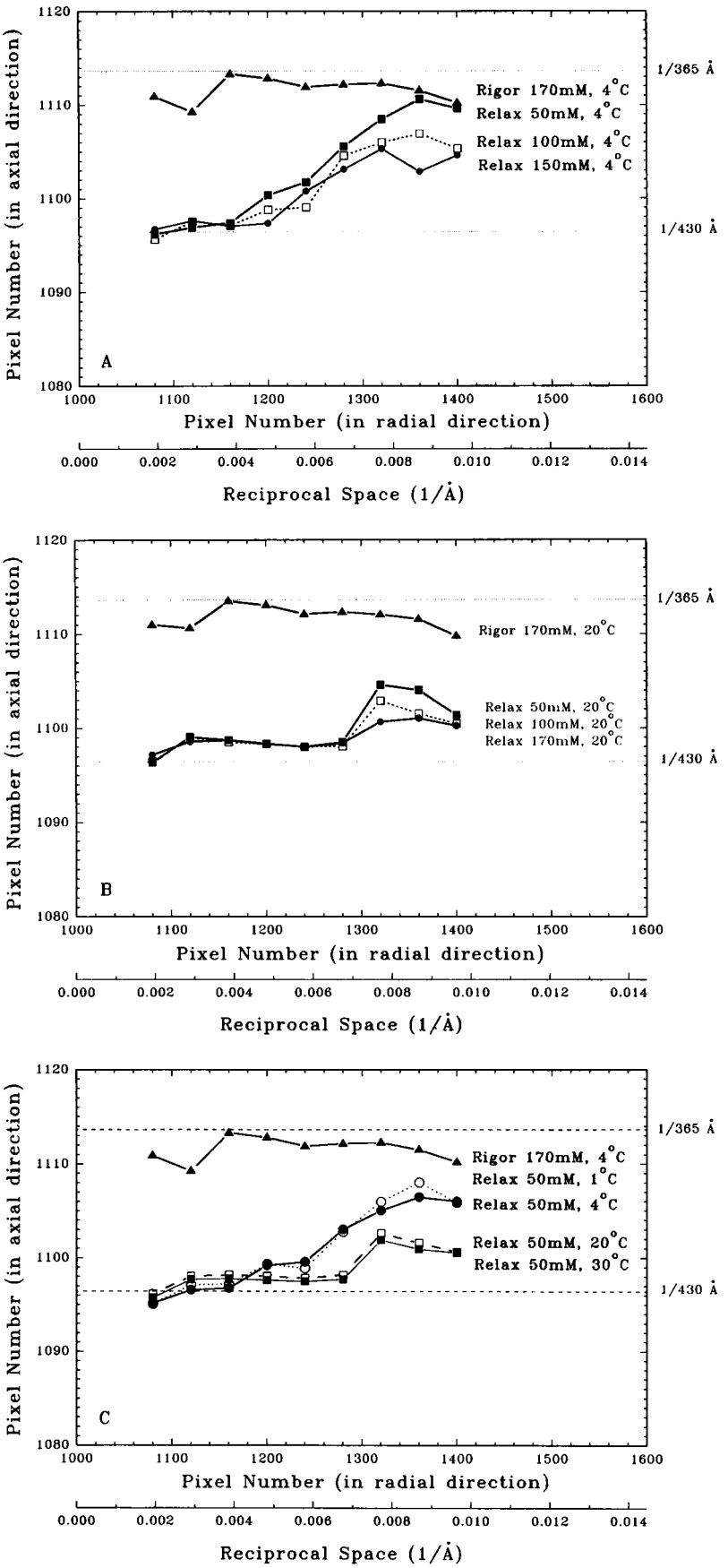

FIGURE 5 Axial centroid position of intensities of the first layer line versus their radial position. (*A*) Temperature = 4°C. Conditions of the muscle: (▲), rigor at 170 mM; (■), relaxed at 50 mM; (□), relaxed at 100 mM; (●), relaxed at 150 mM. (*B*) At 20°C. Conditions of the muscle: (▲), rigor at 170 mM; (■), relaxed at 50 mM; (□), relaxed at 100 mM; (●), relaxed at 170 mM. (*C*) μ = 50 mM for relaxed bundles, at various temperatures: (○), 1°C; (●) 4°C; (□), 20°C; (■), 30°C. (▲) Rigor at 4°C and μ = 170 mM. The shift of the centroids from the first myosin-based layer line spacing toward the first actin-based layer line spacing depends on the ionic strength that parallels the increase in weak attachment of cross-bridges. See text for details.

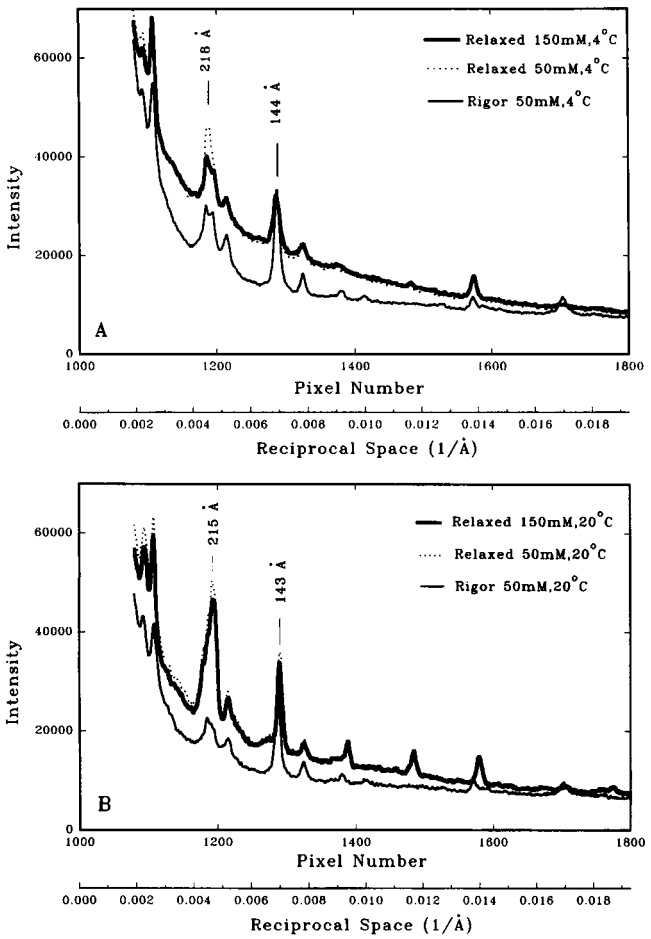

FIGURE 6 Profiles of intensities along the meridian of the diffraction patterns from a single bundle of fibers under various conditions. The background level of the profiles is a measure of the diffuse scattering, originated from the disordered population of the cross-bridges. (*A*) At T = 4°C; (*B*) at T = 20°C. *Thick solid line*, relaxed at μ = 150 mM; *dotted line*, relaxed at 50 mM; *thin solid line*, rigor at 50 mM. Approximately half of the difference in the background between the relaxed fiber at 20°C and rigor is contributed by CPK used in the ATP regenerating system. The data were obtained from the same muscle bundle.

20°C and the rigor condition was due to the scattering by CPK in the relaxing solution. [For the sake of brevity, we shall designate the third myosin filament meridional reflection as the "143 Å" reflection, and the group of reflections centered around the second meridional reflection as the "215 Å" reflections.]

Meridional reflections

To measure the intensities and spacings of myosin-based reflections on the meridian, axial slices along the meridian with a width of 0.0046 $Å^{-1}$ were made. The width used was sufficient to include the entire meridional 143 Å reflection. The integrated intensities and centroids of the peaks are summarized in Table 2.

Spacing changes

It is clear from Table 2 that in the relaxed muscle the spacing of reflection M3 on the meridian increases ~1% (from 143.2 Å to 144.5 Å) upon lowering the temperature from 20°C to 4°C, as reported previously by Lowy et al. (1991). It is noteworthy that the changes in the spacing of the thick filament repeat are associated with temperature changes only, not with any tension generation. It is also interesting to note that at 4°C, in transition from relaxed state to rigor, the spacing of M3 does not change, contrary to earlier reports on frog sartorius muscle (Haselgrove, 1975) and on rabbit muscle at 20°C (Table 1).

The spacings of "215 Å" (M2), 72 Å (M6), and 48 Å (M9) reflections on the meridian show parallel changes (Table 2). The spacings of the myosin-based layer lines appear to shift by the same magnitude. Due to the low intensities, quantitative determination is not as reliable. At a constant temperature, there is no significant difference in those spacings at different ionic strengths.

Under rigor condition, the spacing of the third-order meridional reflection remains at 144.3 Å, regardless of temperature.

Intensity changes

For the relaxed muscles at 4°C, I_{215} increases, whereas I_{143} decreases with decreasing ionic strength from 150 mM to 50 mM (Table 2). In contrast, the rigor muscle at 4°C exhibits low I_{215} and strong I_{143}. This result makes it even less likely that there is an increasing rigor component in the relaxed muscle as the ionic strength is lowered.

For relaxed muscle at 20°C, both I_{215} and I_{143} are stronger relative to those at low temperature (4°C). However, both decrease with increasing ionic strength. The I_{215} and I_{143} of the rigor muscle remain approximately unchanged with temperature.

The intensity changes of the meridional reflection at $1/48$ $Å^{-1}$ (M9) is not parallel to that of (M3) at $1/143$ $Å^{-1}$. As the temperature increased from 4°C to 20°C, I_{48} decreased by 2- to 3-fold, whereas I_{143} increased by ~30% at μ = 150 mM and by ~120% at μ = 50 mM. It suggests that M3 and M9 may originate from different parts of the axially repeating myosin molecules (see also Huxley et al., 1996).

Other notable features

Sampling on the myosin layer lines in the patterns from relaxed muscle

At low temperature and low ionic strength, the filament lattice is well ordered. Under this condition, frequently sampling is observed on the myosin part ($R < 0.005$ $Å^{-1}$) of the first layer line ("M + A") and the second myosin layer line. At higher ionic strengths, similar sampling has been observed, although it has been weaker than that at low ionic strength. Since the sampling is very weak and broad, precise indexing is not yet possible. It appears that the sampling occurs at spacings consistent with a simple lattice,

TABLE 2 Intensities and spacings of myosin-based meridional reflections from skinned fiber bundles

Conditions	T (°C)	μ (mM)	I_{215}*	I_{143}*	I_{72}*	I_{48}*	d_{215} (Å)	d_{143} (Å)	d_{72} (Å)	d_{48} (Å)
Relaxed#	4	50	4.98	1.93	0.96	0.27	218.8	144.6	72.3	47.97
Relaxed§	4	150	3.02	2.43	0.97	0.22	219.0	144.5	72.3	47.96
Relaxed¶	20	50	9.50	4.09	1.21	0.09	215.1	143.1	71.6	47.55
Relaxed‖	20	150	8.10	3.25	1.03	0.09	214.0	143.2	71.5	47.74
Rigor	20	170	1.94	3.35	0.33	0.12	217.9	144.3	72.5	48.25
Rigor	4	170	2.19	3.73	0.35	0.17	217.6	144.2	72.4	48.04

*Intensities from each bundle were normalized with respect to its equatorial intensity I_{10} (= 100) at μ = 50 mM and T = 4°C. The axial width of the slice is 0.0046 Å^{-1}.
#Average of two bundles.
§Average of the same two bundles as in (*).
¶Average of three bundles.
‖Average of the same three bundles as in (¶).

rather than with a super lattice observed in the frog muscle (Huxley and Brown, 1967; Squire, 1981). However, improved counting statistics are needed for definite identification. Interestingly, at 20°C and 30°C, sampling is not discernible on these two layer lines. However, sampling is observable on LL3, and to a lesser extent on LL6. These samplings probably originate from structures other than cross-bridges (see Malinchik et al., 1997). At 4°C, the sampling on LL3 and LL6 is uncertain due to the weak intensities of those layer lines.

Sampling on the actin layer lines under rigor conditions

The sampling on the actin-based layer lines is prominent and more easily identifiable. The sampling appears to be consistent with the spacings of a simple lattice. Temperature does not appear to have an effect on the sampling.

DISCUSSION

The main features of the low-angle x-ray diffraction patterns from chemically skinned relaxed fibers are attributable to a helical arrangement of myosin cross-bridges. These myosin-based reflections are highly temperature-sensitive, as reported previously (Wray, 1987; Wakabayashi et al., 1988; Lowy et al., 1991). At a given temperature, these reflections are not significantly affected by changes in ionic strength. On the other hand, the first actin-based layer line, though very weak under the relaxing conditions, is affected by ionic strength, most likely due to cross-bridge attachment in the weak binding states.

Enhancement of the first actin-based layer line

Further evidence for cross-bridge attachment in the relaxed muscle fibers

Biochemical, mechanical, and equatorial x-ray diffraction studies have amply demonstrated that under relaxing conditions significant fractions of cross-bridges attach weakly to actin, and the association constant is highly ionic-strength sensitive. In the present study, the shift of the centroid of the first layer line ("M + A") from $\approx 1/430$ Å^{-1} toward $1/365$ Å^{-1} at larger radial distances (Figs. 1 and 5) is further evidence for the weak attachment of cross-bridges. In all of the relaxed patterns, including those obtained under physiological conditions as well as at low temperatures, the inner part of the first layer line indexes with the thick filament at $\approx 1/430$ Å^{-1}, but the axial centroid of the layer line shifts toward $1/365$ Å^{-1}, starting approximately at the radial position of $1/250$ Å^{-1}. The simplest explanation for the shift is that the first layer line is actually a composite of two layer lines, i.e., the first myosin-based layer line and the first actin-based layer line. The position of the centroid of the composite layer line is determined by the relative contribution from the two closely spaced layer lines. As the fraction of weakly attached cross-bridges increases with lower temperature or ionic strength, the relative contribution of the two layer lines is increasingly dominated by that of the actin-based layer line. It should be noted that although the shift of the centroid starts at the radial distance of $\approx 1/250$ Å^{-1} (Fig. 5), the actual intensification of the actin filament could start at lower radial distances, since the strong myosin layer line in the low angle region could obscure the contribution from the actin layer line.

Fig. 7 is a theoretical illustration of the concept of a composite layer line by assuming 50% of the cross-bridges being well ordered around the thick filament, and the rest either in complete disorder (orientation angles evenly distributed within a cone of 360°) (Fig. 7 *A*) or being attached to actin with attachment orientations randomly assigned (orientations randomly selected within a cone of ±45°) (Fig. 7 *B*). As a way of illustration for the 4°C data, the center of mass of the myosin heads is assumed to be at an averaged distance of 7.8 nm from the center of the actin filament. A fixed orientation would generate high-intensity actin layer lines. The model shows that a bare actin filament alone (no cross-bridge attachment) could not explain the experimental data, since the radius [~50 Å; Egelman (1985)] and the mass of the actin filament are too small to account for the intensification starting at the radial position of $<1/250$ Å^{-1} (see Fig. 5). With 50% attachment of cross-bridges, the intensity profile along the first layer line is well

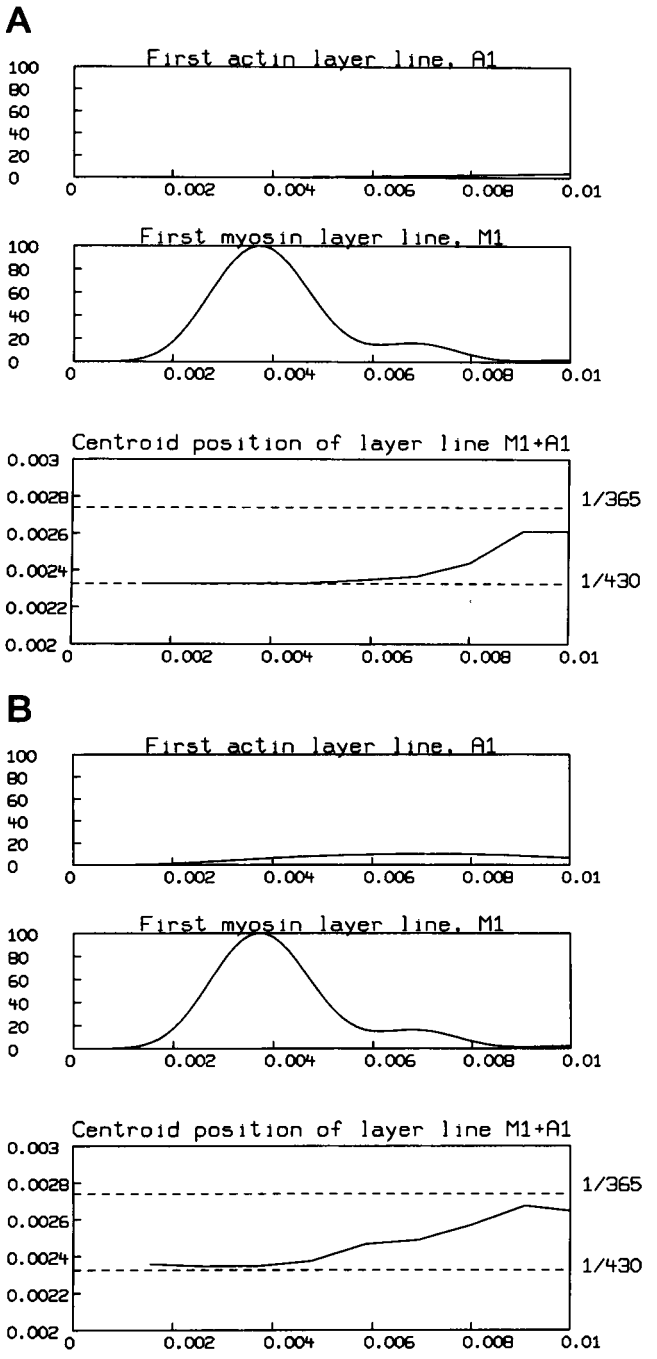

FIGURE 7 Simulation of the unresolved first myosin-actin layer line ("M + A") by modeling. The entire cross-bridge population is assumed to consist of two groups: cross-bridges located on the myosin helix and cross-bridges that are disordered, either (*A*) detached or (*B*) attached. As an illustration, we assume that cross-bridges consist of two myosin heads. Each myosin head approximates the distribution of mass and shape of the crystal structure of Rayment et al. (1993) by 13 spheres. The two myosin heads have an azimuthal angle (β) of 90° (i.e., tangential to the surface of the thick filament) and the two myosin heads are tilted at 20° from each side of the normal to the surface. Their center of mass is located 17.5 nm from the center of the filament. The basic myosin helix has a 429 Å repeat. The actin filament is described in terms of spheres (diameter = 50 Å) on a 13/6 generic helix with a 365 Å repeat (for details of the model, see Malinchik et al., 1997). The cross-bridges from disordered fraction can attach to specific sites on actin monomers along the thin filament, approximately at 30 Å from the center. The attachment is assumed to be site-specific on actin with random orientations within a solid angle cone of ±45° (nonstereospecific) with the center perpendicular to the thin filament axis. The distribution of attachment angle is assumed to be uniform within the cone and zero outside the cone. Intensities of myosin and actin-based layer lines are calculated from cylindrically averaged Fourier transforms of corresponding components, which are then convoluted with symmetrical two-dimensional Gaussian function representing the x-ray beam. To compare with experimental results (Fig. 5), centroid positions from 15 contiguous axial slices along the layer line were calculated, similar to the analysis of experimental data. Fig. 7 *A* shows the resulting centroid positions of the composite layer line with 0% attachment. The actin filament generates the first layer line at $1/365$ Å^{-1} and ordered cross-bridges on myosin helix at $1/429$ Å^{-1}. Fig. 7 *B* shows centroid positions with 50% of cross-bridges attached to actin at random angles. The characteristic axial shift takes place in the region ($\sim 1/250$–$1/125$ Å^{-1}), in agreement with our experimental results, but far from the main maximum arising from the actin filament alone. The modeling supports our interpretation of the experimental data that there is an accretion of mass on the outer surface of the actin filament with the attachment angle being random.

simulated (Fig. 7 *B*) with the centroid spacing starting to shift at 0.005 Å^{-1}, and there is a very slight decrease at ≈ 0.01 Å^{-1}. Thus the modeling supports the idea that the observed shift of the centroid of the first layer line at higher radial distances originates with the attachment of cross-bridges.

Nature of the weak attachment by cross-bridges

There are several features in the diffraction patterns from the relaxed fibers suggesting that the weak attachment of cross-bridges is flexible and nonstereospecific.

The low intensities of actin-based layer lines

Although an intensification of the first actin-based layer line is detected with increasing weak attachment, intensities of the actin-based layer lines are very low overall, in spite of the fact that as much as 60% of the cross-bridges could be attached to actin at 4°C and 50 mM ionic strength (Schoenberg, 1988; Brenner and Yu, 1993). This is in sharp contrast to the patterns obtained under rigor conditions with presumably 100% cross-bridges attached (Cooke and Franks, 1980; Lovell and Harrington, 1981), where the actin layer lines are the dominant feature and the layer lines are clearly indexed with the helical structure of the actin filament. With similar order/stereospecificity of attachment, the intensities of the actin layer lines in relaxed fibers at low ionic strength should be at least 25% of the intensities seen under rigor conditions. As it was first suggested by Xu et al. (1987), the low intensity of the relaxed muscle can be accounted for if the orientation (angle) of weak attachment is disordered and/or if a large amplitude of thermal motion is associated with the attached cross-bridges.

The high level of diffuse scattering

The level of diffuse scattering as indicated by the background intensity (meridional and off-meridional) is signifi-

cantly higher in the relaxed patterns than in the rigor patterns. Since the myosin heads in the skeletal muscle account for ~20% of the total protein mass (Bagshaw, 1993), their order/disorder dominates the diffraction patterns. Therefore, a population of disordered myosin heads could contribute significantly to the diffuse scattering, as suggested by Lowy et al. (Poulsen and Lowy, 1983; Lowy et al., 1991). The present data show that the diffuse scattering is only marginally reduced upon weak attachment (Fig. 6). This is an indication that cross-bridges weakly attached to the thin filament are disordered, with an orientation distribution perhaps hardly distinguishable from the detached myosin heads. This is consistent with the idea of a nonstereospecific attachment where the freedom of movement of the cross-bridges, and/or the distribution of orientations, is not significantly reduced by attachment (Brenner and Yu, 1993). This interpretation is consistent with findings of Xu et al. on frogs (Xu et al., 1987), with EPR studies (Fajer et al., 1991), and with EM studies (Craig et al., 1985; Walker et al., 1995). As a contrast, the diffuse scattering of a muscle in rigor is greatly reduced (Fig. 6), indicating that the freedom of motion/distribution of orientation is restricted, consistent with the idea of a more rigid, stereo-specific attachment.

The cross-bridges are dynamically distributed among three populations

Since it was first proposed by Poulsen and Lowy (1983), there has been substantial experimental evidence (e.g., Lowy et al., 1991) that in a relaxed muscle there are two populations of myosin heads, one helically ordered and one disordered. The present results provide further support for that hypothesis. However, our results add a new dimension to the concept of order-disorder transition: within the disordered population there are the weakly attached and the detached cross-bridges.

Since the order ↔ disorder is completely reversible, the three populations are probably in equilibrium. The relative fraction of cross-bridges ordered (in helix) versus disordered (detached and weakly attached) appears to be primarily affected by temperature (and possibly other variables such as pH). According to our analysis and modeling (Malinchik et al., 1997), the weakening of the myosin-based layer lines and the simultaneous increase of the diffuse scattering (Figs. 1 and 6) is mostly caused by a reduction in the fraction of cross-bridges in the thick filament helical structure, not by an increase in thermal disorder for the population as a whole. Ionic strength at a given temperature, on the other hand, mainly modulates the attachment/detachment distribution within the disordered population. It should be noted that there is a slight increase of intensities of the myosin-based layer lines as the population of weakly attached cross-bridges is increased (Fig. 1 and 6). This finding may appear inconsistent with the concept of three populations in equilibrium. However, lowering the ionic strength per se appears to improve the helical order of the filaments and the lattice order, since the equatorial reflections and all the layer lines are sharper at low ionic strength (Figs. 1 and 2; see also Yu and Brenner, 1989). Such effects appear to be independent of acto-myosin interaction since they occur even at non-overlap sarcomere lengths (>4.2 μm; data not shown). The effects of temperature on the behavior of the cross-bridges also do not appear to depend on the presence of actin (Wray, 1987; Lowy et al., 1991; our own unpublished data). In frog muscle, where the fraction of weakly attached cross-bridges is small, the lowering of ionic strength also increased the intensities of the myosin-based layer lines (Xu et al., 1987). In addition, the weak attachment, even though disordered, may nevertheless stabilize the thermal motion of cross-bridges to some extent, and contribute to the myosin-based intensities more than the detached disordered cross-bridges. Therefore, the present findings are consistent with the concept of cross-bridges being distributed among three populations in equilibrium.

Relation to previous work

Several studies on the structure of skinned relaxed muscle have been reported (Matsuda and Podolsky, 1984; Xu et al., 1987; Wray, 1987; Wakabayashi et al., 1988; Lowy et al., 1991). The present results are in general agreement with the previous work: the myosin-based layer lines are not greatly affected by weak binding of cross-bridges (Matsuda and Podolsky, 1984; Xu et al., 1987) and the myosin layer lines are temperature-sensitive (Wray, 1987; Wakabayashi et al., 1988; Lowy et al., 1991). However, there are several notable differences.

The present relaxed patterns are clearly different from the rigor patterns. Some of the features reported by Matsuda and Podolsky from the relaxed muscle, such as the prominence of the actin-based layer line at 1/69 $Å^{-1}$ and the low meridional intensity of I_{215} are characteristic of rigor patterns and they are absent in the present relaxed patterns. The reason for the discrepancy could be due to the long exposure time used in Matsuda and Podolsky where some degradation of the preparation might have occurred. While the observation that the myosin layer lines were not greatly affected by the weak binding of cross-bridges is confirmed in this study, the intensities of the myosin layer lines are shown to be mainly determined by temperature, not by weak binding cross-bridges. Rather, it is the actin layer lines that are affected by attachment.

Huxley and Brown (1967) described the shift of the first layer line toward the actin-based spacing at higher radial distances in relaxed frog muscle. The intensities at the higher radii were low. It could be that the fraction of weakly attached cross-bridges is small in resting frog muscle. Composite myosin-actin layer lines from activated frog muscle have been observed by Huxley and Brown (1967), by Yagi (1991), and by Bordas et al. (1993). Recently, Lenart et al. (1996) observed intensification of the first actin layer line in frog muscle ~13 ms (at the limit of the time resolution)

after photorelease of Ca^{2+}. The lateral position of the layer line peak shifts toward higher angle during force development, suggesting that the mass of the attached cross-bridges moves toward actin. The question whether the early intensification is related to weak attachment is intriguing, since weak attachment is on the pathway to force generation (Brenner et al., 1991; Kraft et al., 1995).

The temperature sensitivity of the myosin-based layer lines was first reported by Wray (1987), and later by Wakabayashi et al. (1988), and Lowy et al. (1991). The key difference in our result is the intensification of the first actin layer line under a wide range of temperatures that parallels the formation of weakly attached cross-bridges. The thick filament structure as a whole is shown to decrease by $\approx 1\%$ in its repeat as the temperature is raised. The shift is also observed in the layer lines, not limited to meridional reflections as reported previously (Wray, 1987; Lowy et al., 1991).

The order-disorder transition as a function of temperature was analyzed in great detail by Lowy et al. (1991). However, it is suggested in the present study that the diffuse scattering includes contributions from the nonstereospecific *binding* of cross-bridges. Our suggestion of weakly bound cross-bridges being in disorder agrees with an earlier suggestion by Xu et al. (1987).

Our results are consistent with the EPR studies of the skinned fibers, showing that spin labels on the cross-bridges weakly attached to actin are highly mobile and disordered (Fajer et al., 1991). Similarly, EM studies of isolated actin filament with weakly bound S1 also showed random orientations (Craig et al., 1985; Walker et al., 1995). The temperature sensitivity of the myosin helical structure has also been shown in isolated thick filaments (Kensler et al., 1994). At low temperatures the myosin heads are disordered and extend outward from the backbone, whereas at room temperature the myosin heads are arranged in a helix.

The authors thank Dr. Gert Rapp and the technical staff at Hamburg Outstation of European Molecular Biology Laboratory (EMBL) for assisting us in using Beamline X13 at DESY. We thank Dr. Michael Lorenz of Max Plank Institut, Heidelberg, Germany, for providing the source code of Profida. We thank Dr. William Bennett and Max Plank Institut, Hamburg, for use of their image plate scanner Fuji BSA 2000. We also thank Mr. Gary Melvin of the Laboratory of Physical Biology, National Institute of Arthritis and Musculoskeletal and Skin Diseases, National Institutes of Health, for technical assistance throughout different phases of this project.

This work was partially supported by Travel Grant 93-448 from the North Atlantic Treaty Organization, and Deutsche Forschungsgemeinschaft Grant B 849/1-4 to B. Brenner.

REFERENCES

Bagshaw, C. R. 1993. Muscle Contraction. Chapman Hall, London.

Bordas, J., G. Diakum, F. Dias, J. Harries, R. Lewis, J. Lowy, J. G. Mant, M. Fernandez, and E. Towns-Andrews. 1993. Two dimensional time-resolved x-ray diffraction studies of live isometrically contracting frog sartorius muscle. *J. Muscle Res. Cell Motil.* 14:314–324.

Brenner, B., J. M. Chalovich, L. E. Greene, E. Eisenberg, and M. Schoenberg. 1986. Stiffness of skinned rabbit psoas fibers in MgATP and $MgPP_i$ solution. *Biophys. J.* 50:685–691.

Brenner, B., M. Schoenberg, J. M. Chalovich, L. E. Greene, and E. Eisenberg. 1982. Evidence for cross-bridge attachment in relaxed muscle at low ionic strength. *Proc. Natl. Acad. Sci. USA.* 79:7288–7291.

Brenner, B., and L. C. Yu. 1991. Characterization of radial force and radial stiffness in Ca^{2+}-activated skinned fibers of the rabbit psoas muscle. *J. Physiol (Lond.).* 441:703–718.

Brenner, B., and L. C. Yu. 1993. Structural changes in the actomyosin cross-bridges associated with force generation. *Proc. Natl. Acad. Sci. USA.* 90:5252–5256.

Brenner, B., L. C. Yu, and J. M. Chalovich. 1991. Parallel inhibition of active force and relaxed fiber stiffness in skeletal muscle by caldesmon: implications for the pathway to force generation. *Proc. Natl. Acad. Sci. USA.* 88:5739–5743.

Brenner, B., L. C. Yu, and R. J. Podolsky. 1984. X-ray diffraction evidence for cross-bridge formation in relaxed muscle fibers at various ionic strengths. *Biophys. J.* 46:299–306.

Cooke, R., and K. Franks. 1980. All myosin heads form bonds with actin in rigor rabbit skeletal muscle. *Biochemistry.* 19:2265–2269.

Craig, R., L. E. Greene, and E. Eisenberg. 1985. Structure of the actin-myosin complex in the presence of ATP. *Proc. Natl. Acad. Sci. USA.* 82:3247–3251.

Egelman, E. H. 1985. The structure of F-actin. *J. Muscle Res. Cell. Motil.* 6:129–151.

Eisenberg, E., and T. L. Hill. 1985. Muscle contraction and free energy transduction in biological systems. *Science.* 227:999–1006.

Fajer, P., E. A. Fajer, M. Schoenberg, and D. D. Thomas. 1991. Orientational disorder and motion of weakly attached cross-bridges. *Biophys. J.* 60:624–649.

Granzier, H. L., and K. Wang. 1993. Interplay between passive tension and strong and weak binding cross-bridges in insect indirect flight muscle. A functional dissection by gelsolin-mediated thin filament removal. *J. Gen. Physiol.* 101:235–270.

Haselgrove, J. C. 1975. X-ray evidence for conformational changes in the myosin filaments of vertebrate striated muscle. *J. Mol. Biol.* 92:113–143.

Huxley, H. E., and W. Brown. 1967. The low-angle X-ray diagram of vertebrate striated muscle and its behavior during contraction and rigor. *J. Mol. Biol.* 30:383–434.

Huxley, H., A. Stewart, and T. Irving. 1996. X-ray diffraction studies of structural changes in actin and myosin filaments during contraction. *Biophys. J.* 70:41*a*. (Abstr.).

Kensler, R., S. Peterson, and M. Norberg. 1994. The effects of changes in temperature or ionic strength on isolated rabbit and fish skeletal muscle thick filaments. *J. Muscle Res. Cell Motil.* 15:1.

Kraft, T., J. M. Chalovich, L. C. Yu, and B. Brenner. 1995. Parallel inhibition of active force and relaxed fiber stiffness by caldesmon fragments at physiological ionic strength and temperature conditions: additional evidence that weak cross-bridge binding to actin is an essential intermediate for force generation. *Biophys. J.* 68:2404–2418.

Lenart, T. D., J. M. Murray, C. Franzini-Armstrong, and Y. E. Goldman. 1996. Structure and periodicities of cross-bridges in relaxation, in rigor, and during contractions initiated by photolysis of caged Ca^{2+}. *Biophys. J.* 71:2289–2306.

Lovell, S. J., and W. F. Harrington. 1981. Measurement of the fraction of myosin heads bound to actin in rabbit skeletal myofibrils in rigor. *J. Mol. Biol.* 149:659–674.

Lowy, J., D. Popp, and A. A. Stewart. 1991. X-ray studies of order-disorder transitions in the myosin heads of skinned rabbit psoas muscles. *Biophys. J.* 60:812–824.

Malinchik, S., S. Xu, and L. Yu. 1996. Structural transitions in relaxed skinned muscle fiber while changing temperature and ionic strength. *Biophys. J.* 70:161*a*. (Abstr.).

Malinchik, S., S. Xu, and L. Yu. 1997. Temperature-induced structural changes in the myosin thick filament of skinned rabbit psoas muscle. *Biophys. J.* 73:000–000.

Matsuda, T., and R. J. Podolsky. 1984. X-ray evidence for two structural states of the actomyosin cross-bridge in muscle fibers. *Proc. Natl. Acad. Sci. USA.* 81:2364–2368.

Poulsen, F. R., and J. Lowy. 1983. Small angle scattering from myosin heads in relaxed and rigor frog skeletal muscle. *Nature (Lond.).* 303: 146–152.

Rayment, I., W. R. Rypniewski, K. Schmidt-Base, R. Smith, D. R. Tomachik, M. M. Benning, D. A. Winkelman, G. Wesenberg and H. M. Holden. 1993. Three-dimensional structure of myosin-subfragment-1: a molecular motor. *Science.* 261:50–58.

Schoenberg, M. 1988. Characterization of the myosin adenosine triphosphate (M-ATP) crossbridge in rabbit and frog skeletal muscle fibers. *Biophys. J.* 54:135–148.

Squire, J. 1981. The Structural Basis of Muscular Contraction. Plenum Press, New York.

Wakabayashi, T., T. Akiba, K. Hirose, A. Tomioka, M. Tokunaga, C. Suzuki, C. Toyoshima, K. Sutoh, K. Yamamoto, T. Matsumoto, K. Sacki, and Y. Amemiya. 1988. Temperature induced changes of thick filament and location of the functional site of myosin. *In* Molecular Mechanism of Muscle Contraction. H. Sugi and G. H. Pollack, editors. Plenum Publishing Co., New York. 39–48.

Walker, M., J. Trinick, and H. White. 1995. Millisecond time resolution electron cryo-microscopy of the M-ATP transient kinetic state of the acto-myosin ATPase. *Biophys. J.* 68:87S–91S.

Wray, J. 1987. Structure of relaxed myosin filaments in relation to nucleotide state in vertebrate skeletal muscle. *J. Muscle Res. Cell Motil.* 8:62*a*. (Abstr.).

Xu, S., M. Kress, and H. E. Huxley. 1987. X-ray diffraction studies of the structural state of crossbridges in skinned frog sartorius muscle at low ionic strength. *J. Muscle Res. Cell Motil.* 8:39–54.

Xu, S., S. Malinchik, T. Kraft, B. Brenner, and L. C. Yu. 1996. X-ray diffraction evidence that attachment conformation of weakly bound crossbridges in muscle is highly variable (nonstereospecific). *Biophys. J.* 70:290*a*. (Abstr.).

Yagi, N. 1991. Intensification of the first actin layer-line during contraction of frog skeletal muscle. *Ave. Biophys.* 27:35–43.

Yu, L. C., J. E. Hartt, and R. J. Podolsky. 1979. Equatorial x-ray intensities and isometric force levels in frog sartorius muscle. *J. Mol. Biol.* 132: 53–67.

Yu, L. C., and B. Brenner. 1989. Structures of actomyosin crossbridges in relaxed and rigor muscle fibers. *Biophys. J.* 55:441–453.